A Mathematical Model Predicts that Calreticulin Interacts with the Endoplasmic Reticulum Ca^{2+}-ATPase

Helen L. Baker, Rachel J. Errington, Sally C. Davies, and Anthony K. Campbell
Department of Medical Biochemistry, University of Wales College of Medicine, Heath Park, Cardiff CF14 4XN, United Kingdom

ABSTRACT A robust mathematical model developed from single cell calcium (Ca^{2+}) dynamics has enabled us to predict the consequences of over-expression of endoplasmic reticulum-located chaperones. Model predictions concluded that calreticulin interacts with the lumenal domain of the sarcoplasmic and endoplasmic reticulum Ca^{2+}-activated ATPase (SERCA) pump, altering pump affinity for Ca^{2+} ($K_{1/2}$ switches from 247 to 431 nM) and hence generating Ca^{2+} oscillations. Expression of calreticulin in the ER generated an average of six transient-decline oscillations during the Ca^{2+} recovery phase, upon exposure to maximal levels of the agonist ATP. In contrast, normal cells produced a single Ca^{2+} transient with few or no oscillations. By conditioning the model to experimental data, parameters for generation and decay of IP_3 and SERCA pump kinetics were determined. To elucidate the possible source of the oscillatory behavior three possible oscillators, 1) IP_3, 2) IP_3R, and 3) SERCA pump, were investigated and parameters constrained by experimental data to produce the best candidate. Each of the three oscillators generated very good fits with experimental data. However, converting a normal exponential recovery to a transient-decline oscillator predicted that the SERCA pump is the most likely candidate for calreticulin-meditated Ca^{2+} release, highlighting the role of this chaperone as a signal protein within the endoplasmic reticulum.

INTRODUCTION

Calcium (Ca^{2+}) plays a central role in determining cellular activity in animals controlling functions such as contraction, excitability, proliferation, secretion, or cell defense via protein modification or gene expression (Bootman et al., 2001; Campbell, 1983). The eukaryotic cell has two main sources of Ca^{2+}, an influx through channels in the plasma membrane, and release from internal stores, the major store being the endoplasmic reticulum (ER). Ca^{2+} enters the ER through sarcoplasmic and endoplasmic reticulum Ca^{2+}-activated ATPase (SERCA) pumps and is bound to proteins such as calreticulin (CRT) and grp78 (BiP). It is released into the cytosol through inositol 1,4,5 trisphosphate (IP_3) or ryanodine receptors. In cell signaling, much of the focus has been on changes in cytosolic signals that comprise a spatio-temporal pattern leading to different cell responses (Berridge et al., 1998). It is now clear that the cell also has a signaling system within the endoplasmic reticulum (Camacho and Lechleiter, 1995; Llewellyn and Llewelyn-Roderick, 1998; Urano et al., 2000). Here, changes in Ca^{2+} or unfolded protein levels communicate to other parts of the cell, including the nucleus and plasma membrane, to determine whether a cell recovers from stress, crosses a cell cycle checkpoint, or dies by apoptosis. In particular, loss of Ca^{2+} from the ER signals a rapid opening of Ca^{2+} channels in the plasma membrane, leading to a global Ca^{2+} signal and refilling of the ER store. In the longer term, loss of ER Ca^{2+} signals chaperone gene expression and activation of ER proteases (Jeffery et al., 2000). Others, have shown that over-expression of calreticulin alters cytosolic Ca^{2+} signals in a way that cannot be explained by a chaperone acting simply to change store capacity (Lievremont et al., 1997; Llewelyn-Roderick et al., 1998). Thus, if calreticulin is to be a signaling protein within the ER, it must interact with domains facing the inner lumen.

It has been proposed that calreticulin could interact with the IP_3R (Camacho and Lechleiter, 1995) or SERCA 2b (John et al., 1998), the predominant isoform in nonmuscle cells, both of which have potential ER lumenal domains. Three questions now arise: 1) what are the initiating signals within the ER, and how do these communicate throughout the cell; 2) does calreticulin play a role as a signal protein not only storing but controlling Ca^{2+}; and 3) what role do the components, IP_3, the IP_3R, and SERCA pump, play in calreticulin mediated Ca^{2+} responses. This current work focuses on questions 2 and 3.

This paper simplifies the Ca^{2+} mobilization pathway by removing capacitative Ca^{2+} entry and addresses the affect on ER mobilized Ca^{2+}. Thus, our strategy was first to define the effect of calreticulin over-expression on cytosolic Ca^{2+} signals in individual cells and then to develop a mathematical model that predicted the mechanism by which calreticulin caused such changes (Fig. 1). The model has enabled us to assess the relative importance of the two major ER transmembrane regulators of cytosolic Ca^{2+}, the IP_3 receptor, and the SERCA pump in HeLa cells, which have no ryanodine receptors.

Our results show that calreticulin over-expression induces transient-decline oscillations, defined as nonuniform oscillations occurring upon the recovery phase of a single transient. To investigate calreticulin component interactions within the ER, we developed a mechanistic model based

Submitted April 6, 2001, and accepted for publication October 1, 2001.

H. L. Baker and R. J. Errington contribute equally to this paper.

Address reprint requests to Rachel Errington, Department of Medical Biochemistry, University of Wales College of Medicine, Heath Park, Cardiff, CF14 4XN, UK. Tel.: 44-0-2920-742802; Fax: 44-0-2920-745440; E-mail: erringtonrj@cardiff.ac.uk.

0006-3495/02/02/582/09 $2.00

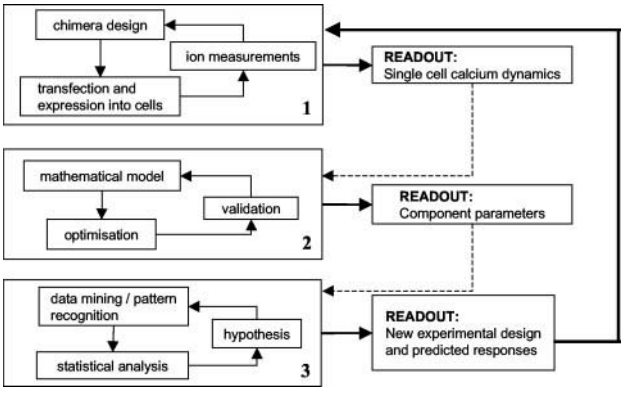

FIGURE 1 Flow diagram demonstrating the central role of mathematical modeling for determining signal protein function. Proposed strategy to incorporate three separate work blocks: 1) manipulation and ion measurement from a cell system, 2) mathematical modeling, and 3) fitting and analysis to investigate the role of ER-signal proteins in calcium mobilization.

initially on the De Young and Keizer (1992) model. Our model was optimized for IP_3 concentration, IP_3R regulation, and SERCA pump activity to minimize the difference between the predicted Ca^{2+} signal and that determined experimentally. Each of the components was restricted by the experimental data, enabling us to determine the most likely candidate for calreticulin-mediated Ca^{2+} oscillations. The results show that each of the three components have oscillatory potential, but highlight for the first time that the SERCA pump is the most likely source for Ca^{2+} oscillations. We show that incorporation of a buffering factor into the model does not affect the qualitative conclusions. The generation of new experimental data, combined with novel mathematics, has predicted an interaction between calreticulin and the SERCA pump, which supports our hypothesis that intralumenal communication within the ER plays a key role in cell signaling.

MATERIALS AND METHODS

Materials

Fura-2 AM was purchased from Molecular Probes (Leiden, Netherlands). A stock was prepared in dimethyl sulfoxide (1 mg/ml). All tissue culture reagents were obtained from Life Technologies/Gibco-BRL (Cleveland, OH) and other reagents unless specified were purchased from Sigma (St. Louis, MO).

Cell culture, loading of Fura-2

Stable transfected HeLa cell cultures with green fluorescent protein (GFP)-calreticulin chimera were routinely grown to 70 to 80% confluency in DMEM supplemented with 10% fetal calf serum 400 μg/ml G418 antibiotic. They were detached from dishes and seeded onto coverslips. Twenty-four hours later the adherent cells were incubated for 20 min in complete DMEM containing 2 μM Fura-2AM at 37°C. The cells were then washed and rested for 10 min in a minimal physiological buffer (10 mM Hepes, pH 7.4, 121 mM NaCl, 5 mM KCl, 0.8 mM $MgCl_2$, 5 mM glucose, and 0.1% bovine serum albumin) containing 1 mM $CaCl_2$ to allow complete cleavage of the ester form of the indicator.

Fluorescent measurement of intracellular calcium

The cover slips were placed into an observation chamber mounted on a Zeiss Axiovert 100. All experiments were performed using a 40×, 1.3 NA oil objective. Ratio images (excitation at 340 and 380 nm; emission at 515 nm) were captured at 2-s intervals using an ORCA-1 cooled CCD camera (Hamamatsu Inc., Welwyn Garden City, UK) from the same field a GFP-calreticulin image was recorded (excitation at 475 nm; emission at 515 nm). The buffer was changed to a calcium-free environment (1 mM EGTA). After 1 min of recording the basal ratio, a supra-maximal concentration of 80 μM ATP was added. Following this, images were acquired for a further 5 min. Separately, the size of the intracellular pool, before and after IP_3-mediated Ca^{2+} release was estimated by the addition of a SERCA pump inhibitor thapsigargin (1 μM). Sequences were acquired and analyzed using AQM-2000 (Kinetic Imaging Inc., Wirral, UK).

Evaluation of calcium recovery characteristics

Individual cells were assigned as either GFP-calreticulin positive (CRT_P) or GFP-calreticulin negative (CRT_N). Data were extracted for each individual wavelength, a background subtracted, and the ratiometric value calculated. Cells (149 CRT_P and 98 CRT_N) were selected from appropriate fields ($n = 18$). The characteristics of each response, the basal ratio (R_{bs}), peak ratio (R_{pk}), and the duration period for the recovery phase (T_d) were determined and number of oscillations (N_{os}) during the recovery period counted for each individual cell. Estimated contribution of the plasma membrane Ca^{2+}-ATPase (PMCA) pump to Ca^{2+} recovery was determined by the amount of Ca^{2+} remaining in the ER pool compared with the amount in the pool to start. This was estimated by calculating the total area under the curve for 39 CRT_P and 34 CRT_N cells after the addition of thapsigargin. Individual cell data for CRT_P and CRT_N cells were pooled to produce mean and standard deviation values, which were compared with a statistical *t*-test.

A linear relationship between experimental fluorescent ratiometric values and Ca^{2+} concentration was assumed. To compare experimental fluorescent data with simulated Ca^{2+} traces both sets of data were normalized to basal levels equal to 1.0.

Modeling of calcium dynamics

A "closed" cell model, which does not include Ca^{2+} influx from the extra-cellular medium, was developed to investigate the effects of calreticulin on the three main components of the Ca^{2+} mobilization pathway: 1) IP_3 production, 2) IP_3 receptor regulation, and 3) SERCA and PMCA pump activity. This model incorporated the De Young and Keizer (1992) equations for Ca^{2+} flow through the IP_3R and input and decay of IP_3. The model considers ER-Ca^{2+} release through the IP_3R (J_{IP_3R}), reuptake via the SERCA pump (J_{SERCA}), and extrusion from the cell by the PMCA pump (J_{PMCA}).

The calcium dynamics for this model are expressed by this ordinary differential equation:

$$\frac{d[Ca^{2+}]_{cyt}}{dt} = J_{IP_3R} - (XJ_{SERCA}) - (YJ_{PMCA}) \qquad (1)$$

in which J denotes the fluxes of processes that increase and decrease cytosolic calcium concentration ($[Ca^{2+}]_{cyt}$), respectively. X denotes the percentage of recycled Ca^{2+} available to reenter the ER, whereas Y denotes the percentage of Ca^{2+} pumped out of the cell.

De Young and Keizer's (1992) equation for Ca^{2+} flow through the IP_3R was included in the model. This equation incorporated calcium dependence on receptor open probability (Bezprozvanny et al., 1991) and IP_3 binding data (Joseph et al., 1989). The flow of Ca^{2+} through the IP_3R is given by:

$$J_{IP_3R} = r_1\left(v_1\left[\frac{[Ca^{2+}]_{cyt}[IP_3]d_2}{([Ca^{2+}]_{cyt}[IP_3] + [IP_3]d_2 + d_1d_2 + [Ca^{2+}]_{cyt}d_3)([Ca^{2+}]_{cyt} + d_5)}\right]^3 + v_2\right)([Ca^{2+}]_{ER} - [Ca^{2+}]_{cyt}) \quad (2)$$

in which r_1 is the ratio of ER to cytosolic volume, v_1 and v_2 are maximal Ca^{2+} fluxes for the IP_3R and the passive leak, and d_1, d_2, d_3, and d_5 are the receptor dissociation constants for IP_3, Ca^{2+} inhibition, IP_3, and Ca^{2+} activation, respectively.

Physiological cytosolic calcium concentration ($[Ca^{2+}]_{cyt}$) is maintained by a combination of sequestration of Ca^{2+} back into the ER via the SERCA pump and extrusion from the cell via the PMCA pump. We have assumed that the PMCA pump has similar kinetic properties to SERCA. Ca^{2+} extrusion via the PMCA and Ca^{2+} uptake by the SERCA pump (Lytton et al., 1992) is governed by this Hill-type equation

$$J_{SERCA/PMCA} = \frac{V_{max}[Ca^{2+}]^n_{cyt}}{[Ca^{2+}]^n_{cyt} + K^n_{1/2}} \quad (3)$$

V_{max} is the maximal activity of the pump, and $K_{1/2}$ is the activation concentration. The Hill coefficient, n, represents the number of cooperative calcium sites required for pump activity.

The model also includes De Young and Keizer's (1992) equation of input and decay for $[IP_3]$:

$$\frac{d[IP_3]}{dt} = I_R([IP_3]^* - [IP_3]) + I_p p(t) \quad (4)$$

in which I_R is the rate constant for loss of IP_3, $[IP_3]^*$ is the steady-state concentration, I_P the pulse amplitude, and $p(t)$ controls the timing of IP_3 pulses denoted by 0 or 1.

Parameter values unless optimized are given in Table 1.

TABLE 1 Model parameter values for the effect of calreticulin on cytosolic Ca^{2+} concentration

Parameter	Value	Description
X	0.4	Recycled Ca^{2+} (%)
Y	0.6	Extruded Ca^{2+} (%)
r_1	0.185	ER vol./Cyt vol.
v_1	6 s^{-1}	Max Ca^{2+} channel flux
v_2	0.11 s^{-1}	Ca^{2+} leak flux
d_1	0.13–2 μM	IP_3 dissociation
d_2	1.05–0.5 μM	Ca^{2+} inhibition dissociation
d_3	9.43.4 nM	IP_3 dissociation
d_5	82.34 nM	Ca^{2+} activation dissociation
$V_{maxSERCA/PMCA}$	Optimized	SERCA/PMCA max Ca^{2+} uptake
$K_{1/2SERCA/PMCA}$	Optimized	SERCA/PMCA activation
I_R	Optimized	Rate constant for IP_3 loss
I_P	Optimized	Pulse amplitude
$[IP_3]^*$	30 nM	Steady state $[IP_3]$
$[Ca^{2+}]_{cyt}$	95 nM	Basal $[Ca^{2+}]_{cyt}$
$[Ca^{2+}]_{ER}$	10 μM	Basal $[Ca^{2+}]_{ER}$
$[IP_3]$	30 nM	Basal $[IP_3]$

Controlling the timing of the oscillator

In all conditions IP_3 must be elevated to release calcium from the ER. It was assumed that the Ca^{2+} transient seen in CRT_N cells was due to IP_3 mediated mobilization of Ca^{2+}; hence one pulse of IP_3 with a 2.5-s duration was required. For each oscillator the onset and duration of each simulated oscillation, governed by the experimental data, was determined using a time dependent oscillatory trace.

IP_3 as the oscillator

IP_3 pulses were regulated according to Eq. 4 where generation and decay of IP_3 was governed by $p(t)$ denoted by 0 or 1. When IP_3 did not act as the oscillator, the IP_3 profile defaulted to that of CRT_N cells (one pulse with a 2.5-s duration).

IP_3R as the oscillator

Opening and closing of the receptor was mimicked by changing the dissociation constants for IP_3 (d_1) and activation by Ca^{2+} (d_2) resulting in a transition from an open to a closed state. Investigation of possible dissociation constants concluded that the best fit could be achieved by switching the dissociation for 1) IP_3 (d_1) between 2 μM and 0.13 μM and 2) activation by Ca^{2+} (d_2) between 0.5 μM and 1.049 μM. When the receptor was not the oscillator it was assumed to remain in a state whereby the channel was open (S_{110}) (De Young and Keizer, 1992).

SERCA as the oscillator

Oscillations from SERCA pump activity were generated by switching the activation concentration ($K_{1/2SERCA}$) between the optimized parameter value (denoted by 1) and a predetermined multiplication factor (1.75), which generated oscillations of the required amplitude.

Effect of buffering on Ca^{2+} model

To implement buffering into the model, we assumed that 90% of Ca^{2+} entering the cytoplasm was immediately absorbed by buffers. As a result the total cytosolic Ca^{2+} flux shown previously in Eq. 1 was multiplied by the factor β (Sneyd et al., 1995) (in which $\beta = 0.1$):

$$\frac{d[Ca^{2+}]_{cyt}}{dt} = \beta(J_{IP_3R} - (XJ_{SERCA}) - (YJ_{PMCA})) \quad (5)$$

Parameter estimation

Computer simulation of the models applied the 4th-order Runge-Kutta method to predict cytosolic Ca^{2+} traces. The system of equations was modeled using the ModelMaker software (Cherwell Scientific, Oxford).

An evaluation of the difference between model simulations and experimental data was applied to adjust selected model parameter values. This adjustment of parameter values was achieved through optimization, apply-

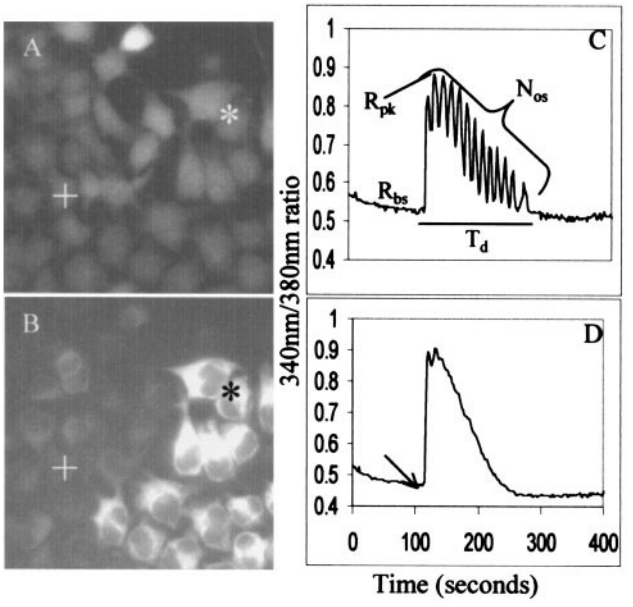

FIGURE 2 Experimental data depicting calcium mobilization. Field of HeLa cells loaded with a calcium indicator Fura-2 (*A*) and the corresponding GFP-calreticulin image (*B*). */+, Represents CRT_P and CRT_N cells, respectively. Cytoplasmic calcium profiles representing ratio (340/380 nm) against time (seconds) for CRT_P (*C*) and CRT_N (*D*) cells. Arrow indicates addition of 80 μM ATP. Measured parameters have been defined as: basal ratio (R_{bs}), peak ratio (R_{pk}), the duration time for the recovery period (T_d), and the number of oscillations during the recovery period (N_{os}) are shown (*C*).

ing the Simplex method, built in to the ModelMaker software, to minimize the difference between predicted and observed values. At the end of each optimization a chi-squared value (an indication of the error between predicted and observed values) was generated. Optimized parameter values were entered into the model and the model reoptimized. This iterative process continued until the chi-squared value did not improve and the visual comparison of simulated overlaid with experimental data was satisfactory.

RESULTS

Effects of calreticulin over-expression on calcium dynamics

The effect of calreticulin over-expression on the calcium recovery profile after mobilization of IP_3-mediated release was measured. To isolate the recovery process from further calcium entry across the plasma membrane all experiments were conducted with HeLa cells in a calcium-free buffer subjected to maximal levels of agonist (80 μM ATP). A typical field of cells (Fig. 2 *a*), containing calreticulin positive cells (CRT_P) and calreticulin negative cells (CRT_N) (Fig. 2 *b*) is shown. Qualitative comparison of calcium dynamics in CRT_N versus CRT_P cells showed a dramatic difference during the recovery phase of the calcium transient. CRT_N cells (Fig. 2 *d*) exhibited a smoothed exponential recovery, whereas an oscillatory pattern was apparent in the CRT_P cells (Fig. 2 *c*). Quantitative analysis of the characteristics defining the calcium recovery profiles (see Fig. 2 *c*) was performed for 149 CRT_P and 98 CRT_N cells. These data were pooled to produce the mean and standard deviation values shown in Table 2. A statistical *t*-test was performed on these data to determine any significant difference between CRT_N and CRT_P cells. This test highlighted no significant difference between basal ratio (R_{bs}), peak ratio (R_{pk}) after addition of ATP and hence peak/basal factor change for CRT_P and CRT_N cells. CRT_P cells were found to have a longer recovery phase (T_d) of ~1.3 fold. CRT_N cells exhibited slight oscillatory behavior located only at the peak of the response (mean $N_{os} = 2 \pm 2$) and rarely during the recovery phase. Whereas CRT_P cells exhibited oscillations throughout the entire recovery period (mean $N_{os} = 6 \pm 2$). Nineteen CRT_N and 14 CRT_P cells were selected to represent the population. A limited model of the system was applied to this group of cells to elucidate interactions between principal components in generating the Ca^{2+} response seen experimentally.

TABLE 2 Quantitative characteristics of calcium recovery

	R_{bs}	R_{pk}	R_{pk}/R_{bs}	T_d	N_{os}
CRT_P	0.6 ± 0.1	1.1 ± 0.3	1.9 ± 0.3	199.3 ± 45.7	6 ± 2
CRT_N	0.5 ± 0.1	1.0 ± 0.2	1.8 ± 0.2	154.9 ± 31.5	2 ± 2

From each experimental plot (see Fig. 2) basic characteristics were extracted: R_{bs}, R_{pk}, T_d, and N_{os}. Mean ± SD values were pooled for CRT_P ($n = 149$) and CRT_N ($n = 98$) cells.

Fitting simulated calcium response to experimental data

An iterative process was implemented to optimize simulated cytosolic Ca^{2+} traces against experimental data. The model focused on the interaction of three key elements: 1) the generation and decay of IP_3; 2) calcium release from the ER through the IP_3R; and 3) calcium reuptake into the ER via the SERCA pump and extrusion from the cell via the PMCA pump. Both the PMCA and the SERCA pump are responsible for removing Ca^{2+} from the cytosol. To ascertain the relative contribution from each pump we determined how much Ca^{2+} was present in the thapsigargin-sensitive pool before and after IP_3-mediated Ca^{2+} release. In these HeLa cells ~60% of calcium was pumped out of the cell via the PMCA pump, while 40% was recycled back into the ER, the relative contributions have been incorporated into the calcium balance equation (Eq. 1). Significantly in this minimal "closed" model the ER store is never completely depleted.

Our implementation enabled, via optimization, the experimental data to influence IP_3 levels and SERCA pump activity. The simulated Ca^{2+} trace for each model was normalized and optimized against the corresponding experimental data. As a result a new set of parameter values were predicted for IP_3 generation and decay (I_P and I_R) and

TABLE 3 Summary of optimized parameter values for all models

	I_P (nM s^{-1})	I_R (s^{-1})	$K_{1/2SERCA}$ (nM)	$V_{maxSERCA}$ (nM s^{-1})	R^2 (%)
CRT_N	92.8 ± 13.5	0.010 ± 0.002	229.4 ± 47.4	237.6 ± 32.3	87.5 ± 4.7
CRT_P (IP_3)	14.7 ± 5.4	0.078 ± 0.034	82.8 ± 29.2	245.3 ± 30.8	93.2 ± 2.1
CRT_P (IP_3R)	266.0 ± 102.4	0.014 ± 0.003	127.5 ± 40.1	210.2 ± 13.0	85.6 ± 4.7
CRT_P (SERCA)	75.9 ± 15.6	0.008 ± 0.002	246.5 ± 56.8	284.3 ± 39.4	89.0 ± 4.6

For 19 CRT_N and 14 CRT_P cells the pulse amplitude (I_P), rate constant for loss of IP_3 (I_R), activation constant for SERCA ($K_{1/2SERCA}$), and maximal Ca^{2+} uptake of the SERCA pump ($V_{maxSERCA}$) were optimized. CRT_P cells were modeled for three conditions: 1) IP_3 oscillating, 2) IP_3R opening and closing, and 3) SERCA sensitivity switching. For each constraint the mean ± SD optimized parameter values were determined. R^2 values were calculated to evaluate the accuracy of the fit along the entire transient.

SERCA pump activity ($K_{1/2SERCA}$ and $V_{maxSERCA}$). The iterative optimization process has been described previously in Materials and Methods.

CRT_N optimizations

Nineteen CRT_N (cells expressing normal levels of calreticulin) models were developed and optimized. For each CRT_N cell, mean, and standard deviation parameter values were pooled (Table 3). To correlate the effectiveness of the fit between simulated and experimental data, R^2 values were calculated where an R^2 value of 100% equals a perfect fit. A typical CRT_N optimized simulation is shown (Fig. 3 *a*), which produced a good fit against its experimental counterpart (mean $R^2 = 88\%$). The optimized parameters for CRT_N cells revealed that on average a single IP_3 pulse with an amplitude (I_P) of 93 nM s^{-1} was required to maintain a Ca^{2+} transient. This IP_3 pulse was degraded at a rate (I_R) of 0.010 s^{-1}. Maximal activity of the SERCA pump ($V_{maxSERCA}$) was optimized with a mean value of 238 nM s^{-1} and a half activation ($K_{1/2SERCA}$) of 229 nM.

The model was then applied to investigate the potential of components of the calcium mobilization pathway to act as possible oscillators. We conducted a series of constrained in silico experiments assigning each component separately as the oscillator and optimizing model parameters against experimental data.

Condition modeling to investigate possible oscillators

Fourteen CRT_P (cells over-expressing GFP-calreticulin) cells were selected, and seven condition-constrained models were developed where we assumed that one, two, or three components had an affect on the response seen. Model simulations for each of these cells were optimized against experimental data to investigate the possible source of the oscillatory behavior seen in Fig. 2 *c*. The three possible components investigated were 1) changeable levels of IP_3 concentration, 2) alternating dissociation constants for IP_3 and activation by Ca^{2+} to mimic opening and closing of the IP_3 receptor, and 3) switching levels of SERCA pump sensitivity, enabling varying pump activity. Of the seven models developed, the closest fit of simulated against experimental data was selected for each of the three oscillatory components, where all of the parameters were optimized.

Optimization of each oscillatory condition model generated a new set of parameter values represented by the mean and standard deviation values pooled for all 14 CRT_P cells (Table 3). A graphical representation of a typical CRT_P cell highlighting the experimental data (Experimental Ca^{2+}), and the effect of the oscillatory components on the simulated cytosolic Ca^{2+} trace (Simulated Ca^{2+}) and the simulated IP_3 trace (Simulated IP_3) are shown in Fig. 3 (*b–d*).

When IP_3 acted as the oscillator a fit with a mean R^2 value of 93% was generated. To achieve this, an amplitude (I_P) of 15 nM s^{-1} was required for each oscillation; this parameter was sixfold lower than that seen for CRT_N cells. An additional consequence of oscillating IP_3 levels was a degradation rate (I_R) eightfold higher than that in CRT_N cells. Maximal Ca^{2+} uptake of the SERCA pump was similar to CRT_N cells ($V_{maxSERCA}$ = 245 nM s^{-1}) with the activation constant ($K_{1/2SERCA}$) 2.8-fold more sensitive.

When opening and closing of the IP_3R generated oscillations optimization resulted in a fit with a mean R^2 value of 86%. To achieve this, more IP_3 (2.8-fold) was produced at the peak compared with CRT_N cells, with a degradation rate 1.3-fold faster. A slight reduction (13%) in the maximal uptake of the SERCA pump ($V_{maxSERCA}$) was seen, whereas the activation constant ($K_{1/2SERCA}$) almost halved. A characteristic of this and other IP_3R versions was an overshoot of oscillations at the top third of the recovery phase.

To enable the SERCA pump to act as the oscillator the activation constant ($K_{1/2SERCA}$) for the pump switched between 247 and 431 nM, generating a fit with an R^2 value of 89%. To achieve this, less IP_3 (20%) was produced (I_P) at the peak compared with CRT_N cells with a degradation rate (I_R) 25% slower. The activation constant for the SERCA pump ($K_{1/2SERCA}$) was similar to CRT_N cells, whereas maximal activity ($V_{maxSERCA}$) increased by 20%.

Summarizing the optimization results for each oscillator IP_3 generated the best fit of experimental and simulated data with an R^2 value of 93% followed by SERCA pump in which $R^2 = 89\%$ then IP_3R $R^2 = 86\%$. A *t*-test comparing the accuracy of the optimization procedure assessing R^2

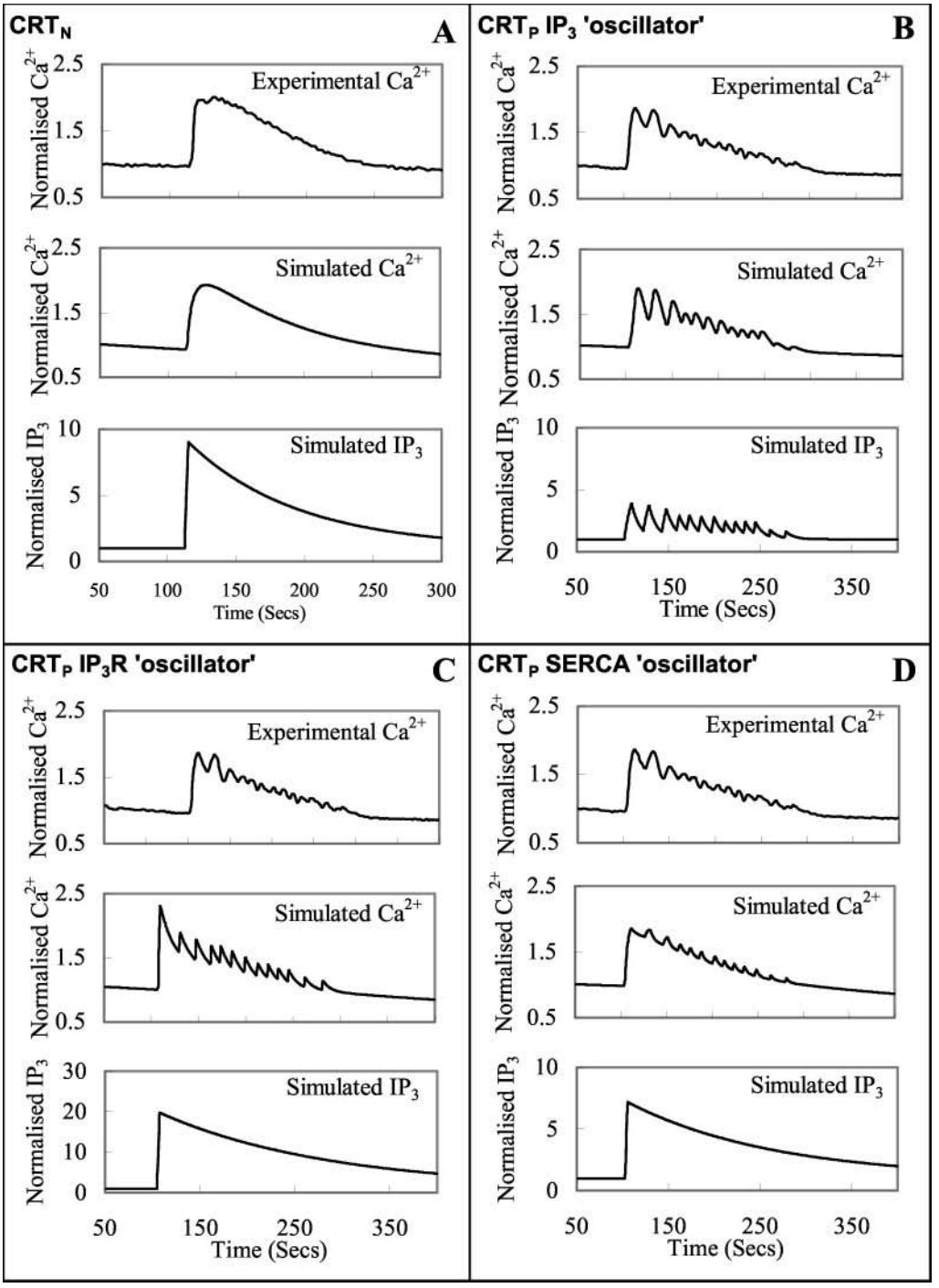

FIGURE 3 Simulation of condition-constrained models. Simulation plots of a typical cell modeled and optimized for the following conditions: CRT_N cell (*A*); CRT_P cell with IP_3 oscillating (*B*); CRT_P cell where IP_3R opens and closes (*C*); and SERCA pump switching (*D*). For each condition, normalized experimental Ca^{2+} (experimental Ca^{2+}), model-simulated Ca^{2+} (simulated Ca^{2+}), and model-simulated IP_3 (simulated IP_3) traces are plotted against time.

values for each of the three oscillating CRT_P conditions highlighted no significant difference between the IP_3R optimizations and those for the SERCA pump. As a result of both of these observations IP_3, IP_3R, and the SERCA pump must all be considered equally as potential oscillators for calreticulin-mediated release.

Effect of adding a buffering factor to the model

It is well established that calcium concentrations are strongly buffered in living cells, but how buffers affect the movement of Ca^{2+} remains unclear. Thus, inclusion of an equation for buffering into mathematical models for

Ca^{2+} oscillations is important. Information on the spatial distribution, timing, and concentration of macromolecules is required to fully understand the role of buffering in cells. However, to a first approximation, buffering can be estimated with the application of a global buffering factor. To elucidate any potential effects of buffering on the current conclusions a buffering factor (Sneyd et al., 1995) in the cytoplasm was added to the model (Eq. 5). Buffering factors ranging from 99% ($\beta = 0.01$) down to 50% ($\beta = 0.5$) of Ca^{2+} buffered in the cytoplasm were considered. A Ca^{2+} buffering factor of 99% ($\beta = 0.01$) was unable to generate oscillations for all conditions before and after parameter optimization, however factors from 90 to 50% produced oscillations before and after optimization. As a result it was assumed that 90% of Ca^{2+} entering the cytoplasm was buffered ($\beta = 0.1$). The model, including buffering, was reoptimized to determine if addition of this factor qualitatively affected the current conclusions. For a given CRT_P cell modeled without buffering and optimized under the three given conditions, 1) IP_3 pulsing (Fig. 3 *b*), 2) IP_3R opening and closing (Fig. 3 *c*), and 3) switching SERCA pump sensitivity (Fig. 3 *d*), the associated R^2 values calculated were 95, 87, and 94%, respectively. For this cell modeled with buffering and reoptimized for all three conditions the R^2 values calculated were 93 (Fig. 4 *b*), 86 (Fig. 4 *c*), and 87% (Fig. 4 *d*). Qualitatively the addition of buffering to the model did not affect the conclusions of this paper; oscillations were generated for all three components therefore, each oscillator still remains a potential candidate for calreticulin-mediated Ca^{2+} oscillations.

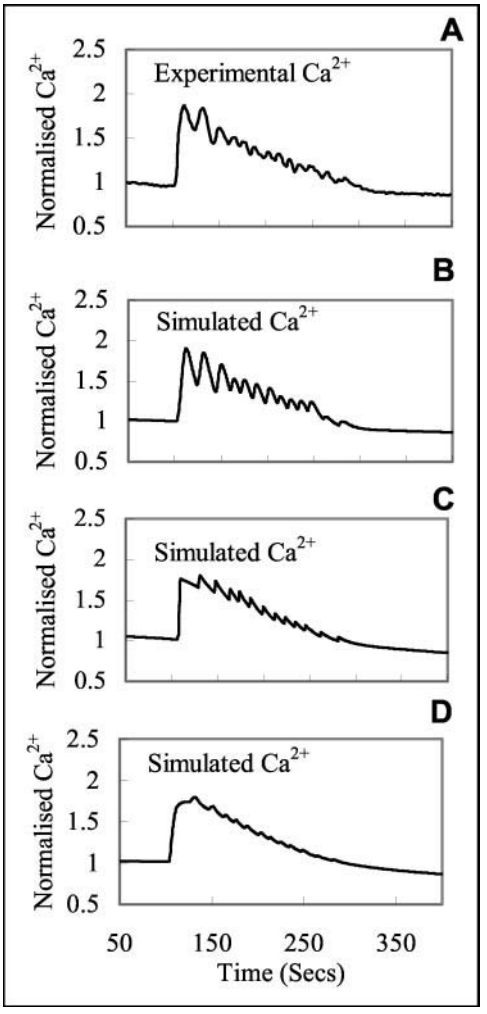

FIGURE 4 Effect of buffering on model optimizations. CRT_P simulation traces after the addition of a buffering factor (β) where 90% of cytosolic Ca^{2+} is buffered ($\beta = 0.1$). (*A*) Experimental trace (experimental Ca^{2+}) for a typical CRT_P cell. (*B–D*) Highlight the same CRT_P cell modeled (simulated Ca^{2+}) for IP_3 pulsing (*B*), IP_3R opening and closing (*C*), and SERCA sensitivity switching (*D*). Plots in these panels (*B–D*) should be compared with those simulated (simulated Ca^{2+}) where buffering has not been included (Fig. 3, *B–D*).

Transforming a CRT_N to a CRTp response

To distinguish between the three components and isolate out the oscillator the outcome from directly translating a CRT_N cell was investigated by applying just the oscillator. At all confidence levels no significant difference between the basal activation constant ($K_{1/2SERCA}$) and the maximal uptake ($V_{maxSERCA}$) of the SERCA pump could be found for CRT_N cells and CRT_P cells where the SERCA pump was the oscillator (Table 3). This led us to investigate whether the main difference between control (CRT_N) cells and those over-expressing calreticulin (CRT_P) was an effect whereby the sensitivity of the SERCA pump switched, resulting in Ca^{2+} oscillations. To achieve this, CRT_P cells were remodeled where only the oscillator was active, all parameter values irrespective of previous optimizations were assigned CRT_N optimized values (Table 2). This would determine whether the imposed oscillatory component alone was able to induce CRT_P behavior. We superimposed the CRT_P simulated traces upon a typical CRT_N experimental trace. This highlighted that IP_3 pulsing (Fig. 5 *b*) or opening and closing of the IP_3R (Fig. 5 *c*) alone was unable to convert a CRT_N to a CRT_P response similar to the experimental traces shown in Fig. 5 *a*. This was achieved, however, by switching the sensitivity of the SERCA pump alone (Fig. 5 *d*). This successful transformation of a CRT_N to a CRT_P cell highlights that the SERCA pump is the most suitable candidate for the Ca^{2+} oscillations seen as a result of over-expression of calreticulin.

DISCUSSION

We demonstrate in the current study that the development and implementation of a mathematical model forms an integral and important tool in the process for determining the role of ER-located signal proteins (Fig. 1). We have

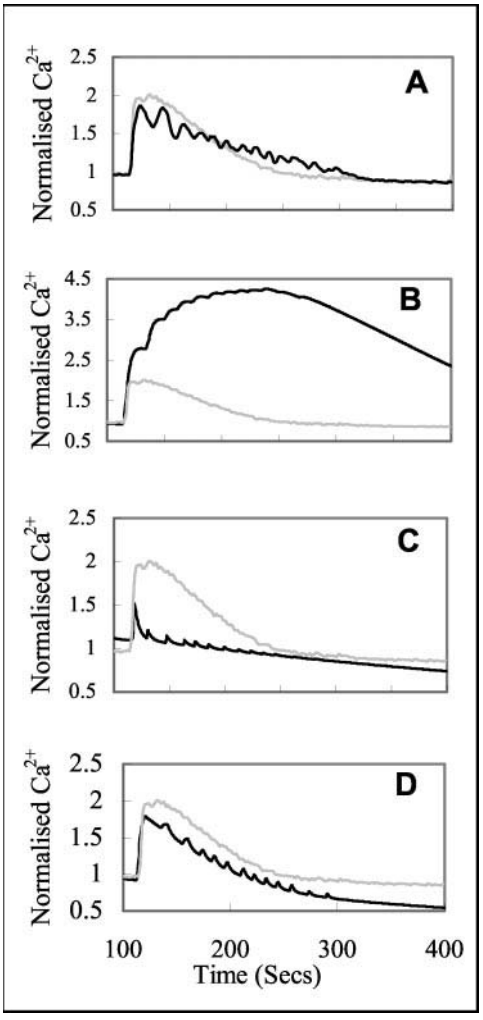

FIGURE 5 Transforming a CRT_N response to a CRT_P. Comparison of normalized CRT_N (*gray lines*) and CRT_P (*black lines*) response profiles against time. (*A*) Typical CRT_N overlaid with a typical CRT_P experimental Ca^{2+} response. (*B–D*) Use the same experimental CRT_N trace and the oscillatory properties of the same CRT_P cell as shown in *A*. (*B*) CRT_N experimental profile compared against a simulated CRT_P trace where only IP_3 oscillates. (*C*) CRT_N experimental trace with a simulated CRT_P profile where only the IP_3R opens and closes. (*D*) CRT_P trace with a simulated CRT_P trace where the sensitivity of the SERCA pump alternates.

shown that over-expression of calreticulin generated a transient decline oscillatory profile not present in control cells and those over-expressing another ER Ca^{2+}-binding chaperone grp78 (BiP) (data not shown). These experimental data have enabled us to predict the oscillatory outcome from each of the components investigated. This highlighted for the first time the potential oscillatory role of the SERCA pump. Conversion of a CRT_N to a CRT_P response has indicated that the SERCA pump is the most likely candidate for calreticulin-mediated Ca^{2+} oscillations. This suggested that the effect of calreticulin was due to a direct interaction with the lumenal domain of an ER protein, and not the direct result of a change in ER free-Ca^{2+} (Llewellyn and Llewelyn-Roderick, 1998). It has been suggested that the SERCA pump may play a role in regulating ER calcium, thereby affecting capacitative calcium entry (Putney, 1986). Our conclusions from the minimal "closed" model supported the hypothesis that signaling within the ER involves interactions between ER Ca^{2+}-binding proteins and other components of the Ca^{2+}-signaling system and that calreticulin acts as a signaling protein.

To identify which of the three potential key candidates were responsible for the transient-decline oscillations, a model based upon the De Young and Keizer (1992) model was applied. The model demonstrated that IP_3 oscillations generated a good fit with experimental data. It has been proposed that IP_3 oscillations may be produced through a positive or negative feedback mechanism incorporating phospholipase C (Cuthbertson and Chay, 1991; Meyer and Stryer, 1991). However, it is unlikely that IP_3 can fluctuate at the rate required to sustain such a calcium profile. Furthermore, there is no obvious direct mechanism whereby calreticulin within the ER could affect IP_3 synthesis or degradation in the cytosol. Thus, the most likely mechanism for transient-decline oscillations may be derived from an interaction between calreticulin and the lumenal domains of either the IP_3R or the SERCA pump. It has been proposed that calreticulin could stabilize the open conformation of the IP_3R prolonging Ca^{2+} release (Camacho and Lechleiter, 1995) or that calreticulin can interact with SERCA2b to inhibit Ca^{2+} uptake (John et al., 1998). It has also been demonstrated that IP_3R subtypes could encode Ca^{2+} oscillatory behavior (Miyakawa et al., 1999). In our optimized model, the SERCA pump and IP_3R generated similar fits of simulated against experimental data. These two potential oscillators were separated by their ability to convert a normal cell recovery profile (CRT_N) to transient-decline oscillations observed in cells over-expressing calreticulin (CRT_P). Thus, this is the first model to propose that the regulation of the SERCA pump can cause cytosolic Ca^{2+} oscillations directly by alternating Ca^{2+} sensitivity for SERCA pump activation. The molecular source of SERCA modulated oscillations now needs to be determined.

The most likely explanation is an on-off binding of calreticulin to the SERCA pump, hence switching its activation state. By identifying and mutating SERCA pump binding sites on calreticulin we can manipulate this potential interaction and measure its downstream effect on calcium mobilization. Additionally, uncaging IP_3 (Fink et al., 1999), using estimates from our model, would provide an elegant approach to separate the contribution of IP_3 pulsing from SERCA switching in calreticulin positive cells.

The simulated model, in general, fitted well with experimental data. However, near the peak the fit deviated slightly, indicating an ill-defined complexity not taken into account by the model. The addition of buffering reduced this deviation where previous fits had overshot. In agreement with previous studies (Wagner and Keizer, 1994) the

effect of a global buffer decreased the amplitude of both the IP_3R and SERCA oscillations. It has previously been shown that oscillatory responses are identical irrespective of the buffering equations applied (Wagner and Keizer, 1994). We selected to implement a global buffer factor (β) (Sneyd et al., 1995) to remove artifacts that may arise from inaccurate parameter estimations. Our qualitative observations were not altered by the inclusion of a buffering factor. The marked decrease in oscillatory amplitude after the inclusion of a buffering factor suggests that an interplay of more than one oscillator either functioning independently during the recovery period or working in concert chaotically or phase dependently would enhance the simulated response. This would require further investigation with particular emphasis on the interaction between the oscillators and their phase relationships.

Our results show how vital it is to combine mathematical modeling with manipulation and measurement of signals in individual living cells if hypotheses in cell signaling are to be properly tested. Ultimately, we can envisage a time-resolved, high-throughput (many manipulations), and high-content (single cell) screening approach to determine the physiological outcome of genetically altered cells, where specific mechanisms are addressed. Mathematical modeling, together with complementary computational methods, will play a central role in the acquisition, mining, and interpretation of such experimental data (Endy and Brent, 2001). Most importantly robust models constructed and developed with "real" data will allow us to predict how intra and extracellular signals are decoded and their effects on cellular outcomes. In this work we have demonstrated the valuable use of a robust mathematical model in elucidating interactions in cell signaling and thus influencing future experimental design. We have shown for the first time that an interaction between calreticulin and the SERCA pump acts as a cause of cytosolic Ca^{2+} oscillations. This extends the role of calreticulin to act as a signal protein in addition to being a storage protein within the ER.

We thank David Llewellyn (Medical Biochemistry, UWCM) for the GFP calreticulin stable cell lines, and we thank Maurice Hallett (Surgery, UWCM) for helpful discussions. This work was funded by a Higher Education Funding Council for Wales/Joint Research Equipment Initiative grant (R.J.E. and S.C.D.) and by Professor G. Elder (Medical Biochemistry, UWCM) (H.L.B.).

REFERENCES

Berridge, M. J., M. D. Bootman, and P. Lipp. 1998. Calcium-a life and death signal. *Nature.* 395:645–648.

Bezprozvanny, I., J. Watras, and B. E. Ehrlich. 1991. Bell-shaped calcium-response curves of Ins(1,4,5)P_3-and calcium gated channels from endoplasmic reticulum of cerebellum. *Nature.* 351:751–754.

Bootman, M. D., T. J. Collins, C. M. Peppiatt, L. S. Prothero, L. MacKenzie, P. De Smet, M. Travers, S. C. Tovey, J. T. Seo, M. J. Berridge, F. Ciccolini, and P. Lipp. 2001. Calcium signalling: an overview. *Semin. Cell Dev. Biol.* 12:3–10.

Camacho, P., and J. D. Lechleiter. 1995. Calreticulin inhibits repetitive intracellular Ca^{2+} waves. *Cell.* 82:765–771.

Campbell, A. K. 1983. Intracellular Calcium: Its Universal Role as Regulator. John Wiley and Sons Limited, Chichester.

Cuthbertson, K. S. R., and T. R. Chay. 1991. Modelling receptor-controlled intracellular calcium oscillations. *Cell Calcium.* 12:97–109.

De Young, G. W., and J. Keizer. 1992. A single-pool inositol 1,4,5-triphosphate-receptor-based model for agonist-stimulated oscillations in Ca^{2+} concentration. *Proc. Natl. Acad. Sci. U. S. A.* 89:9895–9899.

Endy, D., and R. Brent. 2001. Modelling cellular behaviour. *Nature.* 409:391–395.

Fink, C. C., B. Slepchenko, and L. M. Loew. 1999. Determination of time-dependent inositol-1,4,5-trisphosphate concentrations during calcium release in a smooth muscle cell. *Biophys. J.* 77:617–628.

Jeffery, J., J. M. Kendall, and A. K. Campbell. 2000. Apoaequorin monitors degradation of endoplasmic reticulum (ER) proteins initiated by loss of ER Ca^{2+}. *Biochem. Biophys. Res. Commun.* 268:711–715.

John, L. M., J. D. Lechleiter, and P. Camacho. 1998. Differential modulation of SERCA2 isoforms by calreticulin. *J. Cell Biol.* 142:963–973.

Joseph, S. K., H. L. Rice, and J. R. Williamson. 1989. The effect of external calcium and pH on inositol trisphosphate-mediated calcium release from cerebellum microsomal fractions. *Biochem. J.* 258: 261–265.

Lievremont, J.-P., R. Rizzuto, L. Hendershot, and J. Meldolesi. 1997. BiP, a major chaperone protein of the endoplasmic reticulum lumen, plays a direct and important role in the storage of the rapidly exchanging pool of Ca^{2+}. *J. Biol. Chem.* 272:30873–30879.

Llewellyn, D. H., and H. Llewelyn-Roderick. 1998. Overexpression of calreticulin fails to abolish its induction by perturbation of normal ER function. *Biochem. Cell Biol.* 76.

Llewelyn-Roderick, H., D. H. Llewellyn, A. K. Campbell, and J. M. Kendall. 1998. Role of calreticulin in regulating intracellular Ca^{2+} storage and capacitative Ca^{2+} entry in HeLa cells. *Cell Calcium.* 24: 253–262.

Lytton, J., M. Westlin, S. E. Burk, G. E. Shill, and D. H. MacLennan. 1992. Functional comparisons between isoforms of the sarcoplasmic or endoplasmic reticulum family of calcium pumps. *J. Biol. Chem.* 267: 14483–24489.

Meyer, T., and L. Stryer. 1991. Calcium spiking. *Annu. Rev. Biophys. Biophys. Chem.* 20:153–174.

Miyakawa, T., A. Maeda, T. Yamazawa, K. Hirose, T. Kurosaki, and M. Lino. 1999. Encoding of Ca^{2+} signals by differential expression of IP3 receptor subtypes. *EMBO J.* 18:1303–1308.

Putney, J. W. 1986. A model for receptor-regulated calcium entry. *Cell Calcium.* 7:1–12.

Sneyd, J., J. Keizer, and M. J. Sanderson. 1995. Mechanisms of calcium oscillations and waves: a quantitative analysis. *FASEB J.* 9:1463–1472.

Urano, F., A. Bertolotti, and D. Ron. 2000. IRE1 and efferent signaling from the endoplasmic reticulum. *J. Cell Sci.* 113:3697–3702.

Wagner, J., and J. Keizer. 1994. Effects of rapid buffers on Ca^{2+} diffusion and Ca^{2+} oscillations. *Biophys. J.* 67:447–456.